Gaussian-3 Molecular Orbital Study of the Reaction of Boron with Methylamine and the Decomposition Paths of the Reaction Products

Suk Ping So†

Chemistry Department, The Chinese University of Hong Kong, Shatin, N.T., Hong Kong, P. R. China

Received: August 7, 2002; In Final Form: November 6, 2002

G3 molecular orbital calculations predict that the insertions of boron into the CH, NH, and CN bonds of methylamine to form $CH_2(BH)NH_2$, $CH_3N(BH)H$, and CH_3BNH_2 are exothermic by 57.6, 93.9, and 111.8 kcal mol^{-1}, respectively. However, the addition of atomic boron to the N site of methylamine yeilds a weak additon complex CH_3NH_2••B, which is lower in energy than the reactants by only 17.2 kcal mol^{-1}. The dissociation of $CH_3N(BH)H$ to CH_3 and HNBH has a low activation energy of 28.7 kcal mol^{-1} and is the most energetically favored one amomg its three decomposition paths. One of the other two paths yielding the final product CH_3NB has a rate-determining step with a high endothermicity of 111.4 kcal mol^{-1}, but the other leading to CNB has one with a high activation barrier of 105.7 kcal mol^{-1} instead. The conversions of CH_3BNH_2 to the final products CH_2BNH and CH_2BNH_2 are respectively controlled by their endothermicities of 96.9 and 47.7 kcal mol^{-1}.

Introduction

Boron has a very low vapor pressure except at very high temperature. However, laser ablation is a convenient way to produce atomized boron atoms. In addition, these boron atoms may acquire, under the laser-ablation environment, excess kinetic energy, which will increase the probability of their reaction with other molecular species. Accordingly, laser-ablated boron atoms have been found to react readily with various small molecules to produce novel species, which can then be trapped in an argon matrix and studied by FTIR spectroscopy.[1,2] As a result, valuable information for identifying mechanistic pathways may be obtained. Experiments showed that the primary step of the boron−methane reaction is the insertion of a boron atom into the CH bond followed by dehydrogenation to give the novel species $HBCH_2$ and HBCH.[3,4] The boron−ammonia reaction has also been found[5,6] to follow a similar mechanism, namely, insertion of a boron atom into the NH bond to give $HBNH_2$, which then either dissociates to BH and NH_2 or loses a H atom or a H_2 molecule to yeild HBNH or BNH. Besides, the B••NH_3 adduct has been neither observed experimentally nor considered theoretictally. Methylamine has CH and NH bonds as well as a CN bond. Thus, Lanzisera et al.[1] investigated, using the laser-ablation matrix isolation FTIR spectroscopy method, the reaction of boron with methylamine. The aims of their work are to generate some novel molecules, to assess the relative reactivities of the CH, CN, and NH insertion reactions, and to obtain some information about the mechanisms of the reactions. Observed infrared spectra with isotopic boron substitution and theoretical vibrational frequencies of the potential final reaction products computed at the MP2/D95* level of theory have helped to identify CH_3BNH, CH_3NBH, CH_3NB, CH_2BNH_2, CH_2BNH, CH_2NB, HNBH, and CNB as the major species detected spectroscopically. To account for these product molecules, it has been proposed[1] that HNBH is formed from boron insertion into the NH bond of CH_3NH_2 and subsequent CN bond cleavage of the insertion product $CH_3N(BH)H$ (reaction 1), whereas CH_3-NBH, CH_3NB, CH_2NB, and CNB are formed from various dehydrogenations starting from $CH_3N(BH)H$ as shown by reactions 2 and 3. The other products CH_3BNH, CH_2BNH, and CH_2BNH_2 were suggested to be generated from boron insertion into the CN bond of CH_3NH_2 followed by dehydrogenations of the insertion product CH_3BNH_2 as represented by reactions 4 and 5. However, no products formed from boron insertion into the CH bond of CH_3NH_2 (reaction 6) have been identified. In the MP2/D95* calculations of Lanzisera et al.,[1] transition state structures and rate-determining steps associated with the reactions have not been investigated, and the energetic data reported are only the energy changes for the formation of the insertion products $CH_3N(BH)H$, CH_3BNH_2, and $CH_2(BH)NH_2$ from CH_3-NH_2 and B. Hence, it is thought desirable to carry out, as a continuation of our theoretical work on the reaction of boron with methanol,[7] a high level ab initio calculation involving detailed characterization of transition states and rate-determining steps of the above proposed reactions 1−6. In addition, the adduct CH_3NH_2••B has also been examined (reaction 7).

$$CH_3NH_2 + B \longrightarrow CH_3N(BH)H \xrightarrow{(1a)} CH_3 + HNBH \quad (1)$$

$$CH_3N(BH)H \xrightarrow{(2a)} CH_3NBH \xrightarrow{(2b)} CH_3NB \quad (2)$$

$$CH_3N(BH)H \longrightarrow CH_3NBH \xrightarrow{(3b)} CH_2NB \xrightarrow{(3c)} CNB \quad (3)$$

$$CH_3NH_2 + B \longrightarrow CH_3BNH_2 \xrightarrow{(4a)} CH_3BNH \xrightarrow{(4b)} CH_2BNH \quad (4)$$

$$CH_3BNH_2 \xrightarrow{(5a)} CH_2BNH_2 \quad (5)$$

$$CH_3NH_2 + B \longrightarrow CH_2(BH)NH_2 \quad (6)$$

$$CH_3NH_2 + B \longrightarrow CH_2NH_2{\cdot\cdot}B \quad (7)$$

Calculations

The structures of the various species studied were optimized by the energy gradient method at the restricted (for singlet states) and the unrestricted (for doublet states) B3LYP/6-31G* level of theory, using the Gaussian 98 package of programs[8] implemented on our DEC 600 AU, and COMPAQ XP900 and

† Fax: 852-2603-5057. E-mail: sukpingso@cuhk.edu.hk.

10.1021/jp0218241 CCC: \$25.00
Published on Web 02/20/2003

TABLE 1: B3LYP/6-31G* Harmonic Vibrational Frequencies[a] of the Stable ^{11}B-Containing Species Studied

species	frequencies (cm^{-1})
$CH_3N(BH)H$	183.3, 401.6, 476.0, 792.7, 858.0, 1011.8, 1161.1, 1161.5, 1316.8, 1475.5, 1501.2, 1520.9, 1555.0, 2643.8, 3036.9, 3087.5, 3151.7, 3482.6
CH_3BNH_2	121.3, 323.2, 516.5, 533.7, 817.2, 829.9, 886.3, 1076.0, 1339.8, 1397.7, 1486.5, 1503.9, 1646.3, 2993.1, 3074.9, 3097.0, 3476.9, 3635.8
$CH_2(BH)NH_2$	147.7, 353.0, 357.0, 488.1, 746.7, 921.9, 998.9, 1056.4, 1101.2, 1308.4, 1378.7, 1417.7, 1701.2, 2654.3, 2969.7, 2998.4, 3445.5, 3528.2
CH_3NH_2••B	114.5, 230.2, 255.9, 350.1, 972.3, 975.3, 1024.5, 1219.0, 1339.1, 1428.7, 1461.5, 1529.5, 1675.7, 3075.3, 3155.0, 3160.0, 3416.9, 3485.9
HNBH	477.9(464.8)[b], 477.9(464.8), 746.1, 746.1, 1858.3(1819.7, 1825.7), 2919.2, 3889.0(3702.1, 3712.3)
CH_3NBH	270.3, 270.3, 706.5, 706.5, 992.6, 1166.1, 1166.1, 1495.0, 1522.7,1522.7, 2005.6(1975.5), 2919.5, 3024.2, 3079.0, 3079.0
CH_3NB	276.6, 276.6, 999.7, 1160.4, 1160.4, 1492.6, 1521.5, 1521.5, 2058.9 (2020.6), 3024.8, 3081.4, 3081.4
CH_2NB	61.8, 101.3, 1063.7, 1135.7, 1201.4, 1562.5, 1927.0(1836.4), 3034.2, 3102.9
CNB	150.7, 151.1, 1013.2(1016.6), 2132.2(2068.1)
CH_3BNH	323.6, 323.6, 437.0, 437.0, 821.1, 923.4, 923.4, 1374.1, 1497.9, 1497.9, 2024.0(2001.2), 3056.8, 3125.6, 3125.6, 3896.6(3691.1)
CH_2BNH	313.2, 359.5, 395.7, 406.8, 648.8, 878.6, 903.4, 1445.8, 1936.8(1939.3), 3170.0, 3251.7, 3891.3
CH_2BNH_2	311.2, 324.2, 478.7, 690.8, 691.5, 803.2, 938.0, 957.6, 1395.7, 1623.1, 1813.3(1798.5), 3164.6, 3229.9, 3566.1, 3643.3

[a] Not yet uniformly scaled by the factor of 0.96, which is used to calculate ZPEs. [b] Frequencies of observed IR bands for species in argon matrix from ref 1 are in parentheses.

TABLE 2: G3 Total Energies of Species Studied

species	energy (hartrees)
CH_3NH_2 (**1**)	−95.762282
$CH_3N(BH)H$ (**2**)	−120.555190
CH_3BNH_2 (**3**)	−120.583738
$CH_2(BH)NH_2$ (**4**)	−120.497348
CH_3NH_2••B (**5**)	−120.432971
HNBH (**6**)	−80.749278
CH_3NBH (**7**)	−120.013701
CH_3NB (**8**)	−119.335090
CH_2NB (**9**)	−118.721182
CNB (**10**)	−117.517509
CH_3BNH (**11**)	−120.040323
CH_2BNH (**12**)	−119.384832
CH_2BNH_2 (**13**)	−120.006668
CH_3 (**14**)	−39.793618
H_2	−1.167479
B	−24.643219
H	−0.501087
TS1a	−120.509464
TS2a	−120.496383
TS3b	−119.845288
TS3c	−118.588017
TS4a	−120.527160

XP1000 workstations. Various techniques were used to determine transition state structures. Initial geometries were either guessed from the reactant and/or product structures, or located by partial geometry optimization with an appropriate bond held at a series of fixed values. These initial geometries were then fully optimized, i.e., all geometrical parameters allowed to change in value, using the automated TS option of Gaussian 98. (The QST3 option has also been tried in a few cases, but it often yielded no fruitful results.) When the initial symmetry of a species (equilibrium or transition state structure) changed to a practically higher one on geometry optimization, its geometry was then re-optimized under the constraint of the latter symmetry. For example, geometry optimization under C_1 symmetry yielded a nearly C_s structure for the insertion products CH_3BNH_2, $CH_3N(BH)H$, and $CH_2(BH)NH_2$. Hence, they were re-optimized with a C_s symmetry constraint imposed.

The energies of the optimized structures were computed at the Gaussian-3 (G3) theory,[9] which improves significantly over the Gaussian-2 (G2) theory.[10] The conventional G3 method uses a series of QCISDT(FC), MP4SDTQ(FC), and MP2(FU) single-point energy calculations (FC and FU denote "frozen-core" and "full", meaning inclusion of only the valence-shell electrons and of both the inner-shell and valence-shell electrons, respectively) on the MP2(FU)/6-31G* structures with various basis sets (different from those for G2) to approximate a QCISDT(FU)/G3large//MP2(FU)/6-31G* calculation, incorporating a number of correction terms. These include a so-called "higher order correction" based on the number of paired and unpaired valence electrons (with coefficients different from those for G2), scaled (by 0.8929) HF/6-31G* zero-point vibrational energies (ZPEs), spin−orbit corrections (for atomic species only), and so forth.[9] G3 method based, instead, on B3LYP/6-31G* geometries and zero-point vibrational energies scaled by 0.96 has been proposed.[11] In the present work, this modified G3 method was employed because then the $\langle S^2 \rangle$ values obtained for all the doublet structures studied (0.751−0.764) were found to deviate only slightly from the value of 0.75 for a pure doublet state.

Vibrational frequencies were determined by the analytical evaluation of the second derivatives of energy to verify the nature (equilibrium or transition state) of the stationary point structures optimized, to provide zero-point vibrational energy corrections, and to predict vibrational frequencies of the stable species for the sake of their identification by infrared spectroscopy.

The connection between a transition state structure and its reactants and products was established, at the B3LYP/6-31G* level of theory, by the intrinsic reaction coordinate (IRC) calculations based on the reaction path following algorithm of Gonzalez and Schlegel[12,13] as coded in Gaussian 98, or by optimization starting from a transition state structure with one or two of its geometrical parameters distorted.

Results and Discussion

The various stationary point structures studied are depicted in Figures 1 and 2 together with their optimized geometrical parameters. These structures have been shown to be either equilibrium structures (**1**−**14**, Figure 1), or transition state structures (**TS1a**, **TS2a**, **TS3b**, **TS3c**, and **TS4a**, Figure 2) by their B3LYP/6-31G* vibrational frequencies. Table 1 lists the unscaled B3LYP/6-31G* harmonic vibrational frequencies of the stable boron-containing species studied together with experimental values available.[1] Because the observed frequencies are for bands of the species in argon matrix, the agreement between the predicted and the observed frequencies is considered to be reasonable. Table 2 collects the G3 energies of the species studied from which relative energies between various structures can be easily deduced. The energy profiles for the reactions are shown in Figure 3.

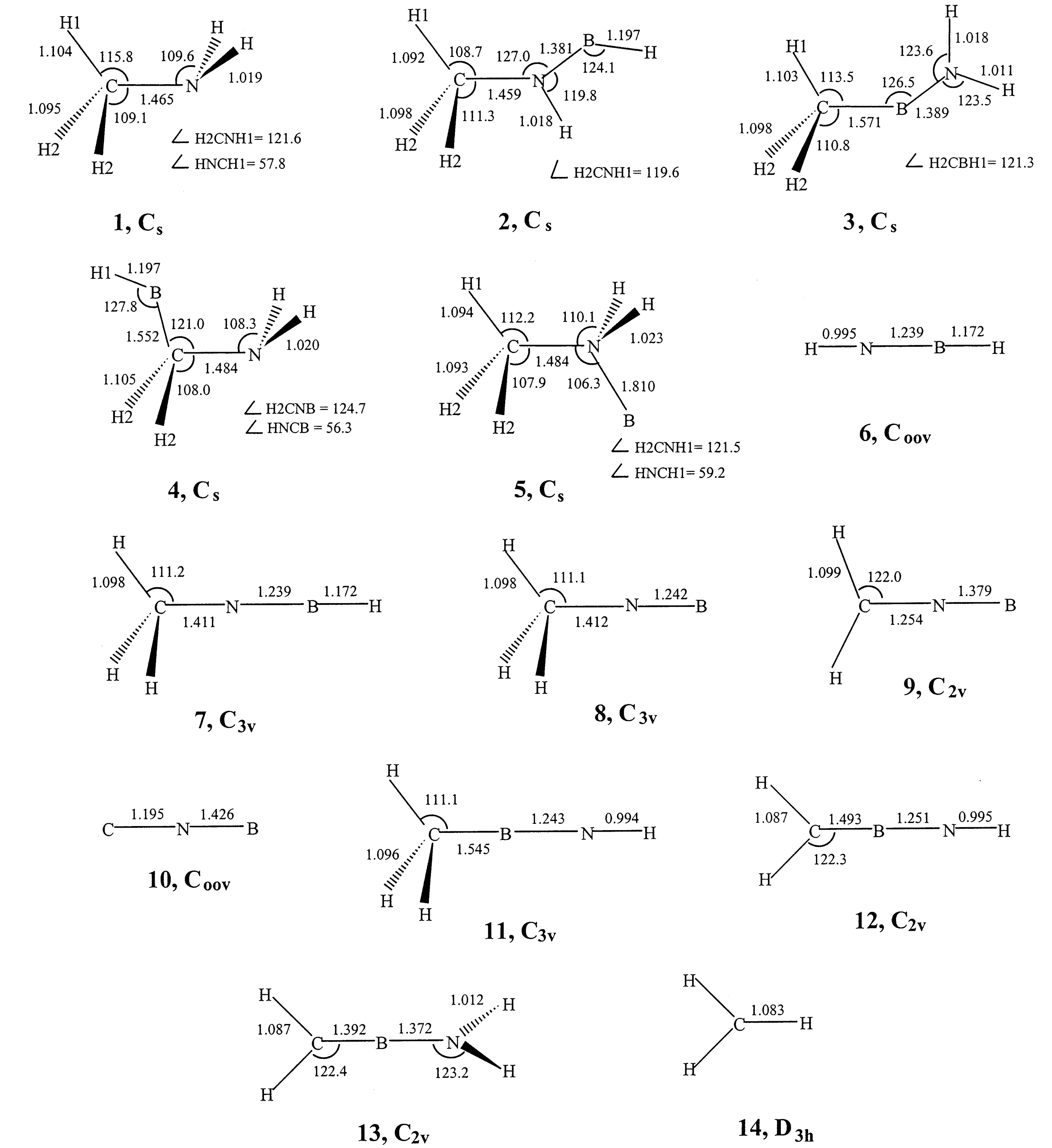

Figure 1. Optimized B3LYP/6-31G* structures of stable species studied. Bond lengths are in angstroms and angles in degrees.

The $\langle S^2 \rangle$ values of the doublet structures computed from their Kohn−Sham orbitals, of which the unrestricted Slater determinants involved in the B3LYP/6-31G* DFT calculations[14−17] are composed, have been found to be $CH_3N(BH)H$ = 0.758, CH_3BNH_2 = 0.752, $CH_2(BH)NH_2$ = 0.751, $CH_3NH_2{\cdot\cdot}B$ = 0.754, CH_3NB = 0.764, CH_2BNH = 0.759, CH_3 = 0.754, **TS1a** = 0.772, **TS2a** = 0.765, and **TS4a** = 0.760. These values are almost identical to or deviate only slightly from the value of 0.75 of a pure doublet state. Hence, for these species, the unpredictable spin contamination effect due to unrestricted wave functions on molecular geometry[18] may be neglected.

It is interesting to note from Figure 1 that, at the B3LYP/6-31G* level, the geometrical parameters of the CH_3 groups of $CH_3N(BH)H$, CH_3BNH_2, and $CH_3NH_2{\cdot\cdot}B$, the NH_2 groups of $CH_2(BH)NH_2$ and $CH_3NH_2{\cdot\cdot}B$, and the CN bonds of $CH_3N(BH)H$, $CH_2(BH)NH_2$, and $CH_3NH_2{\cdot\cdot}B$ have values only slightly different (by 0.019 Å and 3.6° or less) from the corresponding ones of the free CH_3NH_2 subunit. On the other hand, the unique H1CN angle of $CH_3N(BH)H$ has a deviation as large as 7.1° and the NH_2 group becomes nearly trigonal planar in CH_3BNH_2. The calculated XBY (X, Y = H, C, N) bond angle lies between 124.1 and 127.8° for the three insertion products $CH_3N(BH)H$, CH_3BNH_2, and $CH_2(BH)NH_2$ but is 180° for the equilibrium structures HNBH, CH_3NBH, CH_3BNH, CH_2BNH, and CH_2BNH_2. This shows that the boron atom has sp^2 hybridized bonding orbitals in the former three structures but

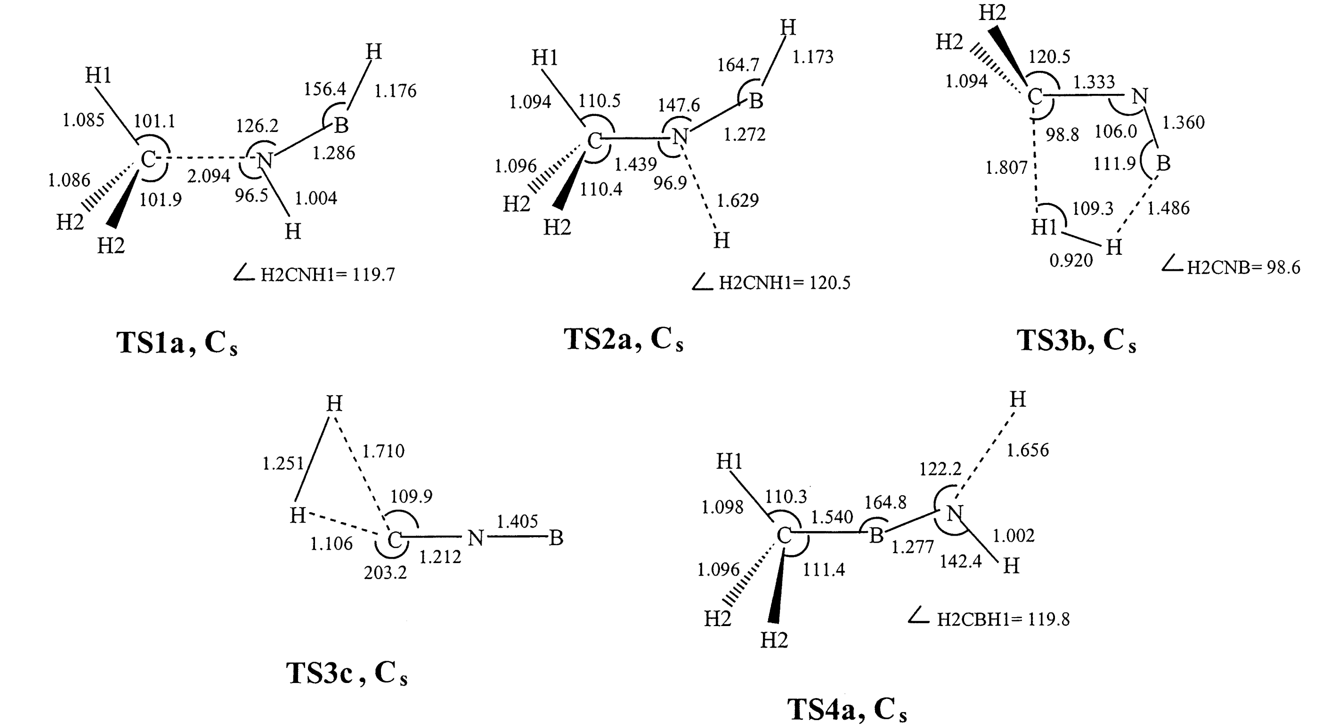

Figure 2. Optimized B3LYP/6-31G* transition state structures of reactions studied. Bond lengths are in angstroms and angles in degrees.

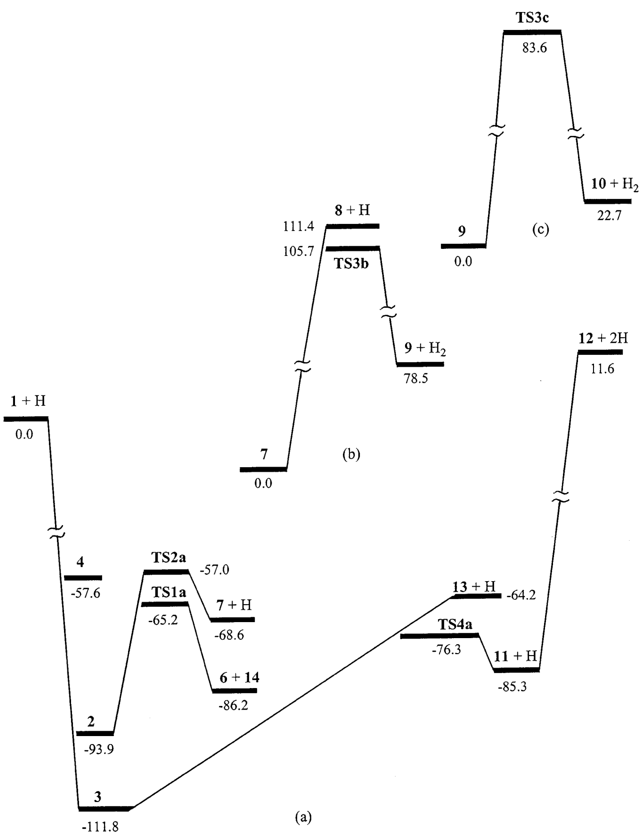

Figure 3. Schematic potential energy profiles of reactions studied. Relative energies are in kcal mol^{-1}.

sp hybridized bonding orbitals in the latter five. Comparison of the calculated BH, BC, and BN bond lengths with the sums of the corresponding atomic radii[19] (single/double/triple bond radius: H = 0.30/−/− Å, B = 0.81/0.71/0.64 Å, C = 0.77/0.67/0.60 Å, and N = 0.74/0.62/0.55 Å) and the corresponding experimental bond distances in some boron compounds[19,20] (e.g., BH = 1.23 Å for BH, t-BH = 1.19 Å for B_2H_6, BC = 1.56 Å for $B(CH_3)_3$, BN = 1.44 Å for $B_3N_3H_6$ (a graphite structure), and BN = 1.28 Å for BN) leads to the following observations:

(1) The BH bonds of $CH_3N(BH)H$, $CH_2(BH)NH_2$, HNBH, and CH_3NBH (1.172−1.197 Å) are single bonds.

(2) The BC bonds of CH_3BNH_2, $CH_2(BH)NH_2$, and CH_3-BNH (1.545−1.571 Å) are single bonds, that of CH_2BNH (1.493) has some double bond character, and that of CH_2BNH_2 (1.392 Å) is a double bond.

(3) The BN bonds of $CH_3N(BH)H$, CH_3BNH_2, CH_2NB, and CH_2BNH_2 (1.372−1.389 Å) are double bonds. However, the BN bond of CNB (1.426 Å) has some single bond character, those of HNBH, CH_3NBH, CH_3NB, CH_3BNH, and CH_2BNH (1.239−1.251 Å) are partially triple bonds, and that of CH_3-NH_2••B (1.810 Å) is substantially longer than a single bond.

A boron atom has the electronic configuration $1s^22s^22p^1$ and a maximum valence of 3. In the G2 study of the reaction of boron with methanol,[7] the BC bond of the reaction product CH_2-BOH and the BO bonds of CH_3BO, CH_2BO, and HBO have been found to be unexpectedly short (shorter than a single and a double bond, respectively). This has been attributed to the overlapping of the filled nonbonding pπ orbital of the C or O atom with the vacant pπ orbital of the B atom. Furthermore, the ionic-covalent resonance of the bond and the incomplete octet of the B atom have been considered[21,22] to be additional factors for the shortness of the BX (X = O, F, Cl, Br) bonds in BR_3 compounds. Obviously, these reasons can also account for the unexpectedly short BC bond of CH_2BNH_2 and the BN bonds of HNBH, CH_3NBH, CH_3NB, CH_3BNH, and CH_2BNH predicted above in the present G3 calculation though a N atom instead of an O atom is now involved. This conclusion is evidenced by the relatively large Mulliken overlap populations[23] of these bonds as listed in Table 3. Besides, the AOM (atomic overlap matrix)-derived covalent bond orders calculated by the AIM (atom in molecules) method[24,25] are also shown. For polarized bonds, the computed covalent bond orders will be

TABLE 3: Mulliken Overlap Populations[a] and AOM-Derived Covalent Bond Orders of Some Bonds of Species Studied

species		BC	BN	CN	BH
CH_3NH_2 (**1**)	Pop:			0.657(0.029)	
	Ord:			1.049	
$CH_3N(BH)H$ (**2**)	Pop:		1.016(0.346)	0.632(0.010)	0.740
	Ord:		0.851	1.004	0.717
CH_3BNH_2 (**3**)	Pop:	0.807(0.043)	0.951(0.313)		
	Ord:	0.668	0.799		
$CH_2(BH)NH_2$ (**4**)	Pop:	0.852(0.073)		0.646(0.004)	0.652
	Ord:	0.753		1.080	0.761
HNBH (**6**)	Pop:		1.618(0.935)		0.818
	Ord:		1.107		0.714
CH_3NBH (**7**)	Pop:		1.686(0.951)	0.586(0.072)	0.815
	Ord:		1.119	0.985	0.724
CH_3NB (**8**)	Pop:		1.694(0.945)	0.551(0.068)	
	Ord:		1.402	0.980	
CH_2NB (**9**)	Pop:		0.743(0.430)	0.889(0.526)	
	Ord:		0.922	1.615	
CNB (**10**)	Pop:		0.493(0.272)	1.024(0.785)	
	Ord:		0.768	1.764	
CH_3BNH (**11**)	Pop:	0.859(0.053)	1.592(0.931)		
	Ord:	0.638	1.021		
CH_2BNH (**12**)	Pop:	0.998(0.185)	1.518(0.861)		
	Ord:	0.675	0.983		
CH_2BNH_2 (**13**)	Pop:	1.461(0.598)	1.026(0.331)		
	Ord:	1.049	0.646		

[a] π-components are in parentheses.

smaller, by variable amounts, than the values anticipated from chemical intuition for purely covalent bonds.[25] Thus, the bond orders in Table 3 indicate that the bonds considered are partially ionic to various degrees. Nevertheless, it should be mentioned that the exact values of the overlap populations and bond orders of Table 3 should not be taken too literally and overemphasized.

The insertion reactions of boron into the NH, CN, and CH bonds of methylamine have been computed to yield the products $CH_3N(BH)H$, CH_3BNH_2, and $CH_2(BH)NH_2$ of C_s symmetry. The transition state structures of these reactions have been searched for at the B3LYP/6-31G* level but, unfortunately, could not be characterized. Thus, no definite conclusions on the barriers of these insertion reactions can be made. The insertion products CH_3BNH_2, $CH_3N(BH)H$, and $CH_2(BH)NH_2$ are predicted to be lower in energy than the reactants (CH_3NH_2 + B) by 111.8, 93.9, and 57.6 kcal mol^{-1} at the G3 level (115.9, 92.8, and 56.3 kcal mol^{-1} at the G2 level for the corresponding insertion products of boron into methanol[7]), respectively. Hence, the insertion reactions studied are exothermic. The present theoretical prediction that the CH bond insertion reaction is the thermodynamically least favored reaction among the three is in line with the fact that no products formed from the decompostion of $CH_2(BH)NH_2$ have been identified in the FTIR experiment.[1] Hence, in view of the FTIR results, the much smaller exothermicity of the reaction, and the larger bond energy (average bond energies:[19] CH = 98.8, NH = 93.4, and CN = 69.7 kcal mol^{-1}), the CH bond insertion reaction may be considered relatively much less important in comparison with the other two insertion reactions and is thus neglected in the boron−methylamine reaction, as in the case of the boron−methanol reaction.[7]

In addition to the insertion reactions considered above, atomic boron (with empty 2p orbitals) may add onto the N site (with a lone pair) of methylamine. The attack is found to be roughly in the direction of the nitrogen lone pair (Figure 1). Optimizations with a series of fixed BN distances show that as the BN distance decreases from 7.0 Å the energy of the (CH_3NH_2 + B) system decreases, leading to the formation of the adduct CH_3NH_2••B without a barrier. This adduct is predicted at the G3 level of theory to lie only 17.2 kcal mol^{-1} below the reactants (CH_3NH_2 + B), and to have an exceptionally long BN bond (1.810 Å) with a very small overlap population of −0.143 and covalent bond order of 0.056. It is thus thought more appropriate to regard CH_3NH_2••B as a weak atom−molecule complex rather a normal species. Attempts to locate transition states for the isomerization of CH_3NH_2••B to the insertion products were not successful. Hence, CH_3NH_2••B is not further considered in this work because of reasons similar to those mentioned above for the case of the CH insertion product and its potential low stability in the energetic laser-ablation environment due to its small binding energy of 17.2 kcal mol^{-1}.

The dissociation of the NH bond insertion product $CH_3N(BH)H$ into CH_3 and HNBH (reaction step 1a) has been found to be endothermic by 7.7 kcal mol^{-1} at the G3 level and to proceed via a transition state structure **TS1a** with a low activation barrier of 28.7 kcal mol^{-1}. It is seen from Figure 1 that the CH, BN, and BH bond lengths of **TS1a** are much closer to the corresponding bond lengths of the dissociation products CH_3 and HNBH rather than those of the reactant $CH_3N(BH)H$. Hence, **TS1a** is a late transition state structure.

The NH bond insertion product $CH_3N(BH)H$ can have other decomposition paths in addition to the CN bond cleavage reaction (reaction 1) as described above. Alternatively, $CH_3N(BH)H$ may first be converted to CH_3NBH by a H(N) elimination (reaction step 2a). This reaction has been found to be endothermic by 25.4 kcal mol^{-1} and to proceed via a transition state **TS2a** with a barrier of 36.9 kcal mol^{-1} at the G3 level. Again, **TS2a** is seen from Figures 1 and 2 to be a late rather than an early transition state structure. The reaction product CH_3NBH formed above can then yield either CH_3NB by a H(B) elimination (reaction step 2b) or CH_2NB and finally CNB by H_2 eliminations (reaction steps 3b and 3c). The reaction step 2b is predicted here to have no activation barrier but a high endothermicity of 111.4 kcal mol^{-1}. This step is therefore the rate-determining step of reaction 2 in the generation of the final product CH_3NB. Reaction steps 3b and 3c are, however, found to go through transition states **TS3b** and **TS3c** with barriers of 105.7 and 83.6 kcal mol^{-1} and to be endothermic by 78.5 and 22.7 kcal mol^{-1}, respectively. Thus, the rate-determining step of reaction 3 in yeilding the final product CNB is 3b. As a result, reaction steps 2b and 3b are almost equally feasible energywise, and among the three decomposition paths of $CH_3N(BH)H$ considered, reaction 1 is the most energetically favored one. It is interesting to note that **TS3b** has a five-membered ring and H_2 is eliminated from CH_2NB asymmetrically as shown in **TS3c**. Data in Figures 1 and 2 show that the HCN angle and the BN bond of **TS3b** are closer in value to the corresponding parameters of the product CH_2NB than those of the reactant CH_3NBH. Similarly, the CN and BN bond lengths of **TS3c** lie also closer to those of the product CNB. Hence, **TS3b** and **TS3c** are late transition state structures.

The CN bond insertion product CH_3BNH_2 may be converted by the elimination of an amino hydrogen to CH_3BNH (reaction step 4a) which may then lose a methyl hydrogen to give the final product CH_2BNH (reaction step 4b). Alternatively, CH_3BNH_2 may be transformed to the product CH_2BNH_2 by a H(C) elimination (reaction step 5a). The present G3 work shows that reaction 4a proceeds via a transition state structure **TS4a** with an activation barrier of 35.5 kcal mol^{-1}. On the other hand, both reactions 4b and 5a are endothermic reactions with no activation barrier. Their respective endothermicities are 96.9 and 47.7 kcal mol^{-1}. Thus, the rate-determining step of reaction 4 in yielding CH_2BNH is 4b. Geometrical data shown in Figures

1 and 2 indicate **TS4a** to be also a late transition state structure. Results in Figure 1 and Table 3 reveal that, on losing a H atom in reactions 4a and 5a, CH_3BNH_2 undergoes the following major changes: the electrons redistribute themselves in such a way that the BN double bond becomes partially triple in the product CH_3BNH of the former reaction and the BC single bond changes to a double bond in the product CH_2BNH_2 of the latter reaction. It is commonly known that the larger the electronegativity difference of two atoms, the larger the ionic resonance energy of the bond formed betwwen them[19] The elctronegativities of boron, carbon, and nitrogen are 2.0, 2.5, and 3.0, respectively.[19] It may thus be speculated that the formation of a BN partially triple bond probably lowers, in part at least, the energy of CH_3-BNH to such an extent that a barrier appears in the H(N)-elimination reaction of CH_3BNH_2.

As noted above, the BC/BN/CN bond characters are roughly single/partially triple/− in CH_3BNH, partially double/partially triple/− in CH_2BNH, single/double/− in CH_3BNH_2, double/double/− in CH_2BNH_2, −/double/single in $CH_3N(BH)H$, and −/partially triple/partially double in CH_3NBH (Figure 1 and Table 3). Hence, in terms of π-bond or electron delocalization effect, the product CH_2BNH of the methyl hydrogen elimination reaction 4b is less stabilized or even not stabilized over its reactant CH_3BNH in comparison with the stabilization of CH_2-BNH_2 over CH_3BNH_2 of the similar reaction 5a. On the other hand, the products CH_3NBH and CH_3BNH of the amino hydrogen eliminations 2a and 4a are seen to be stabilized to similar extends over their respective reactants $CH_3N(BH)H$ and CH_3BNH_2. This may attribute, partly at least, to the above prediction of this work that reaction 5a has an endothermicity (47.7 kcal mol^{-1}) only about half of that of reaction 4b (96.9 kcal mol^{-1}) but reactions 2a and 4a have similar endothermicities (36.9 and 35.5 kcal mol^{-1}).

Acknowledgment. I thank my department for a financial allocation and my university for a Special Equipment Grant to support the acquisition of the workstations.

References and Notes

(1) Lanzisera, D. V.; Andrews, L. *J. Phys. Chem. A* **1997**, *101*, 824 and references cited.

(2) Lanzisera, D. V.; Andrews, L. *J. Phys. Chem. A* **1997**, *101*, 1482.

(3) Hassanzadeh, P.; Andrews, L. *J. Am. Chem. Soc.* **1992**, *114*, 9239.

(4) Hassanzadeh, P.; Hannachi, Y.; Andrews, L. *J. Phys. Chem.* **1993**, *97*, 6418.

(5) Thompson, C. A.; Andrews, L. *J. Am. Chem. Soc.* **1995**, *117*, 10125.

(6) Thompson, C. A.; Andrews, L.; Martin, J. M. L.; El-Yazal, J. *J. Phys. Chem.* **1995**, *99*, 13839.

(7) So, S. P. *J. Phys. Chem. A* **2002**, *106*, 3181.

(8) Frisch, M. J.; Trucks, G. W.; Schlegel, H. B.; Scuseria, G. E.; Robb, M. A.; Cheeseman, J. R.; Zakrzewski, V. G.; Montgomery, J. A., Jr.; Stratmann, R. E.; Burant, J. C.; Dapprich, S.; Millam, J. M.; Daniels, A. D.; Kudin, K. N.; Strain, M. C.; Farkas, O.; Tomasi, J.; Barone, V.; Cossi, M.; Cammi, R.; Mennucci, B.; Pomelli, C.; Adamo, C.; Clifford, S.; Ochterski, J.; Petersson, G. A.; Ayala, P. Y.; Cui, Q.; Morokuma, K.; Malick, D. K.; Rabuck, A. D.; Raghavachari, K.; Foresman, J. B.; Cioslowski, J.; Ortiz, J. V.; Stefanov, B. B.; Liu, G.; Liashenko, A.; Piskorz, P.; Komaromi, I.; Gomperts, R.; Martin, R. L.; Fox, D. J.; Keith, T.; Al-Laham, M. A.; Peng, C. Y.; Nanayakkara, A.; Gonzalez, C.; Challacombe, M.; Gill, P. M. W.; Johnson, B. G.; Chen, W.; Wong, M. W.; Andres, J. L.; Head-Gordon, M.; Replogle, E. S.; Pople, J. A. *Gaussian 98*, revision A.7; Gaussian, Inc.: Pittsburgh, PA, 1998.

(9) Curtiss, L. A.; Raghavachari, K.; Redfern, P. C.; Rassolov, V.; Pople, J. A. *J. Chem. Phys.* **1998**, *109*, 7764.

(10) Curtiss, L. A.; Raghavachari, K.; Trucks, G. W.; Pople, J. A. *J. Chem. Phys.* **1991**, *94*, 7221.

(11) Baboul, A. G.; Curtiss, L. A.; Redfern, P. C.; Raghavachari, K. *J. Chem. Phys*. **1999**, *110*, 7650.

(12) Gonzalez, C.; Schlegel, H. B. *J. Chem. Phys.* **1989**, *90*, 2154.

(13) Gonzalez, C.; Schlegel, H. B. *J. Chem. Phys.* **1990**, *94*, 5523.

(14) Kohn, W.; Sham, L. J. *Phys. Rev. A* **1965**, *140*, 1133.

(15) Ziegler, T. *Chem. Rev.* **1991**, *91*, 651.

(16) Johnson, B. G.; Gill, P. M. W.; Pople, J. A. *J. Chem. Phys.* **1993**, *98*, 5612 and references cited.

(17) Wang, J. H.; Becke, A. D.; Smith, V. H. *J. Chem. Phys.* **1995**, *102*, 3477.

(18) McDouall, J. J. W.; Schlegel, H. B. *J. Chem. Phys.* **1989**, *90*, 2363.

(19) Pauling, L. *The Nature of the Chemical Bond*, 3rd ed.; Cornell University Press: Ithaca, NY, 1960.

(20) Gray, H. B. *Electrons and Chemical Bonding*, W. A. Benjamin, Inc.:New York, 1965 (see also references therein).

(21) Cotton, F. A.; Wilkinson, G. *Advanced Inorganic Chemistry*, 3rd ed.; Interscience Publishers: NY, 1972.

(22) Bachler, V.; Metzler-Nolte, N. *Eur. J. Inorg. Chem.* **1998**, 733.

(23) Mulliken, R. S. *J. Chem. Phys.* **1955**, *23*, 1833, 1841.

(24) Bader, R. F. W. *Atoms in Molecules: A Quantum Theory*; Oxford University Press: Oxford, U.K., 1990.

(25) Cioslowski, J.; Mixon, S. T. *J. Am. Chem. Soc.* **1991**, *113*, 4142 and references cited.